Finger formation at the base of ash clouds: A linear stability analysis

Paul Jarvis [1] Jonathon Lemus [1] Allan Fries [1]
Amanda Clarke [2] Jeremy Phillips [3] Costanza Bonadonna [1]

[1]Section of Earth and Environmental Sciences, University of Geneva

[2]School of Earth and Space Exploration, Arizona State University

[3]School of Earth Sciences, University of Bristol

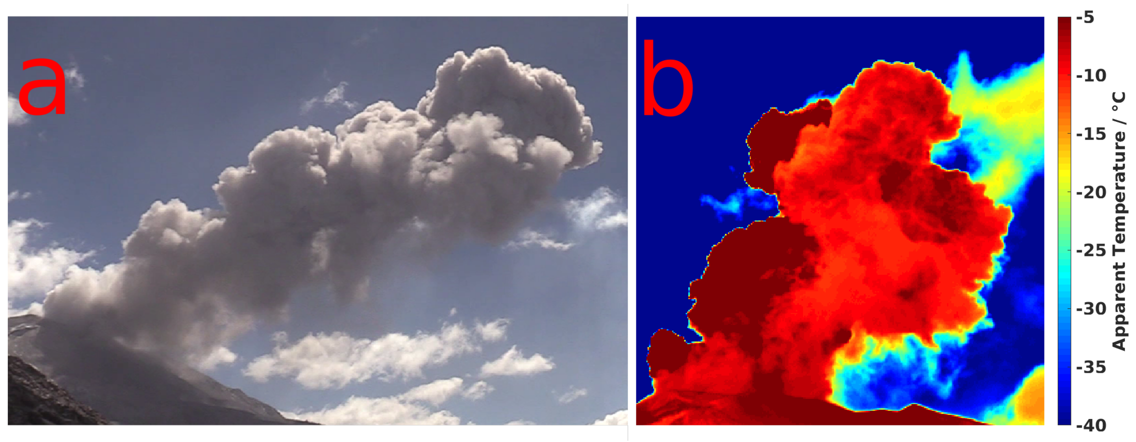

Figure 1. a) Visible and b) infrared images of ash clouds from Vulcanian explosions of Sabancaya volcano, Peru. Fingers can be seen in both images.

Introduction

Volcanic ash presents a hazard for infrastructure and human health. Understanding ash settling is therefore crucial for assessing the associated risk. Downard-propagating fingers(Figure 1), hypothesised to form from a gravitational instability at the base of the ash cloud (Figure 2) have been seen at many volcanoes, and in analogue experiments (**Allan Fries**) and numerical models (**Jonathon Lemus**). Here we present a linear stability analysis, that predicts the initial growth rate of the fingers.

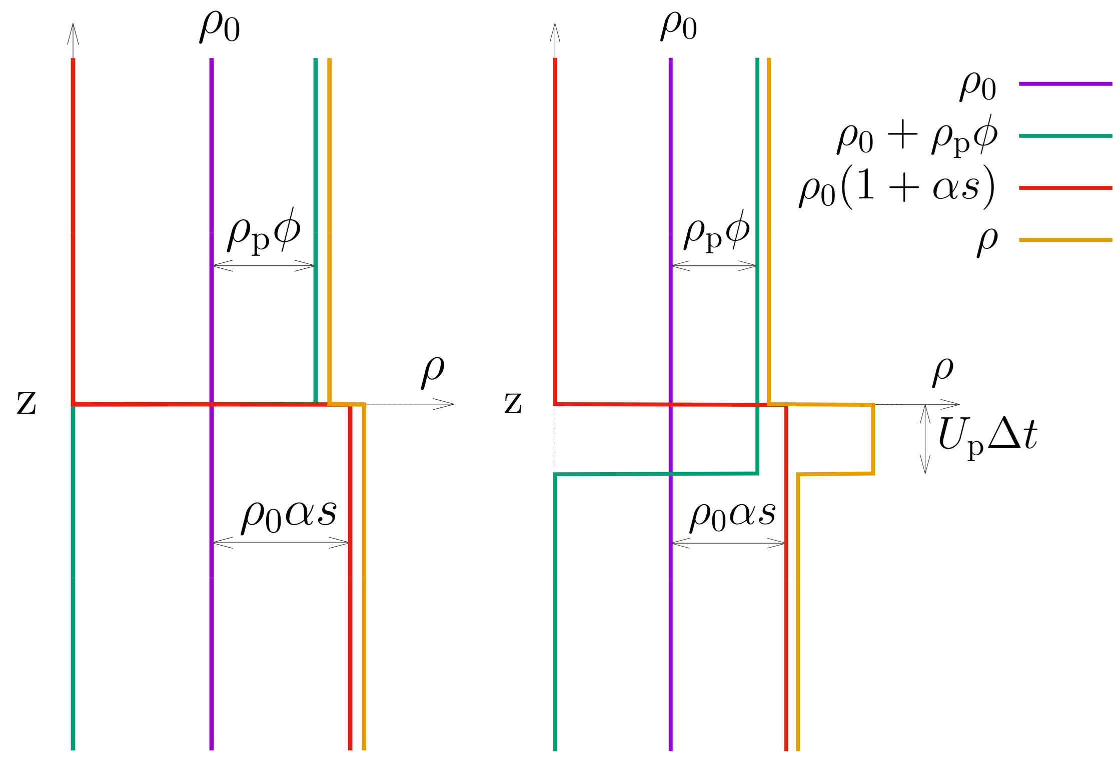

Figure 2. Despite an initial stable configuration, ash settling leads to the formation of a gravitationally unstable **particle boundary layer**.

Equations of motion

Expansion

	Equation of motion	Expansion
Conservation of mass	$\nabla\cdot\mathbf{u}(\mathbf{x},t)$	$\mathbf{u}(\mathbf{x},t)=\hat{\mathbf{u}}(z)e^{i(k_x x+k_y y-\omega t)}$
Conservation of momentum	$\frac{\partial\mathbf{u}(\mathbf{x},t)}{\partial t}+[\mathbf{u}(\mathbf{x},t)]\cdot\nabla]\mathbf{u}(\mathbf{x},t)=\frac{\nabla P(\mathbf{x},t)}{\rho_0}+\nu\nabla^2\mathbf{u}(\mathbf{x},t)-g'\hat{\mathbf{z}}$	$P(\mathbf{x},t)=P^{(0)}(\mathbf{x},t)+\hat{P}(z)e^{i(kx-\omega t)}$
Conservation of particles	$\frac{\partial\phi(\mathbf{x},t)}{\partial t}+[\mathbf{u}(\mathbf{x},t)]-\mathbf{U}_\mathsf{p}]\cdot\nabla\phi(\mathbf{x},t)=D_\mathsf{p}\nabla^2\phi(\mathbf{x},t)$	$\phi(\mathbf{x},t)=\phi^{(0)}(\mathbf{x},t)+\hat{\phi}(z)e^{i(kx-\omega t)}$
Conservation of solute	$\frac{\partial s(\mathbf{x},t)}{\partial t}+\mathbf{u}(\mathbf{x},t)x\cdot\nabla s(\mathbf{x},t)=D_\mathsf{s}\nabla^2 s(\mathbf{x},t)$	$s(\mathbf{x},t)=s^{(0)}(\mathbf{x},t)+\hat{s}(z)e^{i(kx-\omega t)}$
Reduced gravity	$g'=g\left(1+\alpha s(\mathbf{x},t)+\frac{\rho_p\phi(\mathbf{x},t)}{\rho_0}\right)$	$\hat{P}\ll P^{(0)},\hat{\phi}\ll\phi^{(0)},\hat{s}\ll s^{(0)}$

Unknowns		Parameters	
$\mathbf{u}(\mathbf{x},t)$	Fluid velocity	ρ_0	Reference fluid density
$P(\mathbf{x},t)$	Pressure	ν	Kinematic viscosity
$\phi(\mathbf{x},t)$	Particle volume	$\mathbf{U}_\mathsf{p}$	Particle settling velocity
$s(\mathbf{x},t)$	Solute concentration	ρ_p	Particle density
Variables		D_p	Particle diffusivity
$\mathbf{x}$	Position vector	D_s	Solute diffusivity
t	time	g	Gravity
$\hat{\mathbf{z}}$	Vertical unit vector	α	Expansivity

Base states

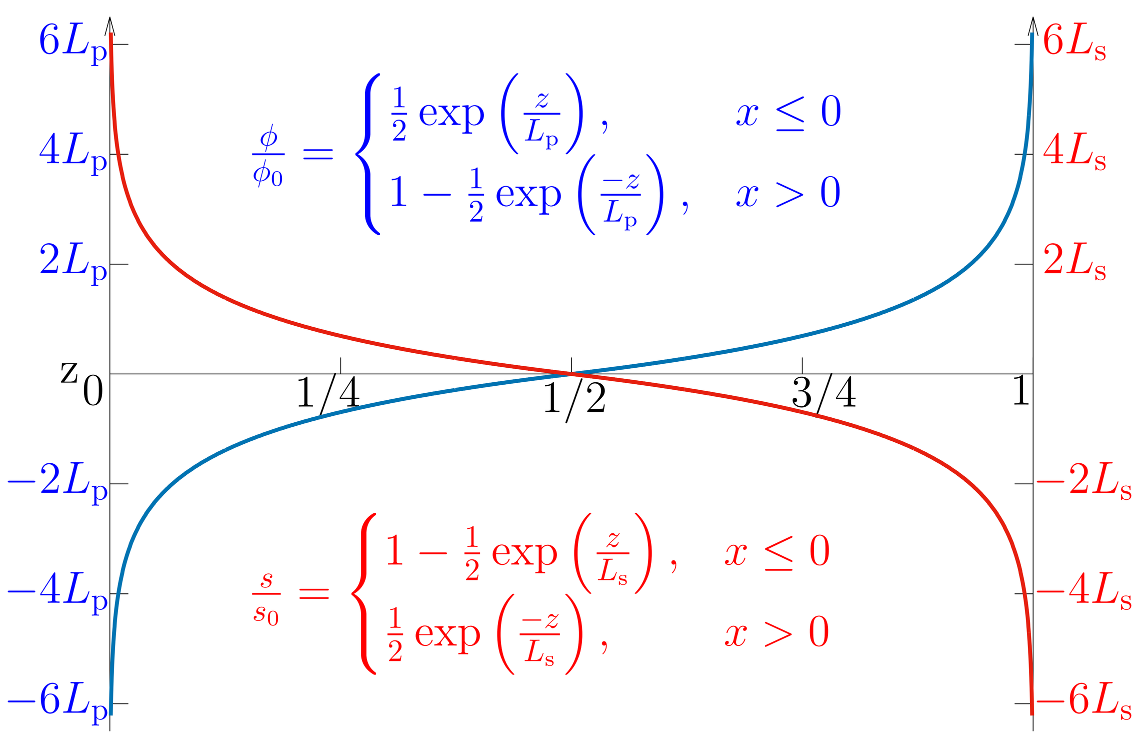

Figure 3. Choice of base states for the particle and solute concentrations. The transitions have length scales L_p and L_s respectively.

Non-dimensionalisation and generalised eigenvalue problem

We nondimensionalise the system using the characteristic length and velocity scales

$$L_\mathsf{c}=L_\mathsf{p}\qquad U_\mathsf{c}=\frac{gL_\mathsf{p}^2}{\nu}$$

This gives seven dimensionless parameters

$$Re=\frac{gL_\mathsf{p}^3}{\nu^2},\quad U'_\mathsf{p}=\frac{\nu U_\mathsf{p}}{gL_\mathsf{p}^2}\quad L'_\mathsf{s}=\frac{L_\mathsf{s}}{L_\mathsf{p}}$$

$$A_\beta=\frac{\alpha s_0\nu^2}{gL_\mathsf{p}^3},\quad A_\gamma=\frac{\rho_\mathsf{p}\nu^2}{gL_\mathsf{p}^3\rho_0}\quad Sc_\mathsf{s}=\frac{\nu}{D_\mathsf{s}},\quad Sc_\mathsf{p}=\frac{\nu}{D_\mathsf{p}}$$

Can express problem as a generalised eigenvalue equation

$$\begin{pmatrix}\frac{1}{Re}\left(\frac{\mathrm{d}^4}{\mathrm{d}z'^4}-2k'^2\frac{\mathrm{d}^2}{\mathrm{d}z'^2}+k'^4\right) & k'^2A_\beta & k'^2A_\gamma\\ \frac{\partial s^{(0)}}{\partial z'} & \frac{1}{ReSc_\mathsf{s}}\left(k'^2-\frac{\mathrm{d}^2}{\mathrm{d}z'^2}\right) & 0\\ \frac{\partial\phi^{(0)}}{\partial z'} & 0 & \frac{1}{ReSc_\mathsf{p}}\left(k'^2-\frac{\mathrm{d}^2}{\mathrm{d}z'^2}\right)-U'_\mathsf{p}\frac{\mathrm{d}}{\mathrm{d}z'}\end{pmatrix}\begin{pmatrix}\hat{u_z}\\ \hat{s}\\ \hat{\phi}\end{pmatrix}=i\omega\begin{pmatrix}\left(\frac{\mathrm{d}^2}{k'^2-\mathrm{d}z'^2}\right) & 0 & 0\\ 0 & 1 & 0\\ 0 & 0 & 1\end{pmatrix}\begin{pmatrix}\hat{u_z}\\ \hat{s}\\ \hat{\phi}\end{pmatrix}$$

This is a generalised eigenvalue problem and is solved for the eigenvalue $\omega=\Omega+i\sigma$. Solutions where $\sigma<0$ are unstable, and the associated growth rate is $|\sigma|$. We can therefore predict the fastest growing perturbation wavelength $\lambda_\mathsf{max}=2\pi/k_\mathsf{max}$ which maximises $|\sigma|$ for different values of the dimensionless parameters.

Special case: Rayleigh-Taylor instability

To validate the model, we consider the special case of a single phase ($s_0=0$) in the absense of a settling velocity ($U'_\mathsf{p}=0$). This reduces the problem to that of the well studied Rayleigh-Taylor problem.

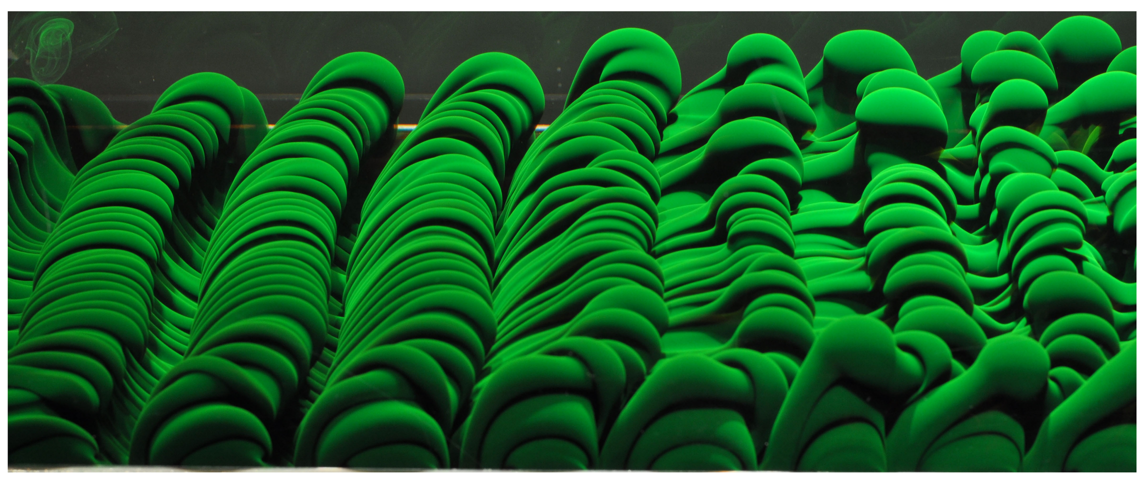

Figure 4. Experimentally produced Rayleigh-Taylor instability. The green fluid is lighter than the overlying clear fluid. Credit: Megan Davies Wykes

Choose sufficiently large $Re(10^4)$ and $Sc_\mathsf{p}(10^3)$ that system becomes independent of them

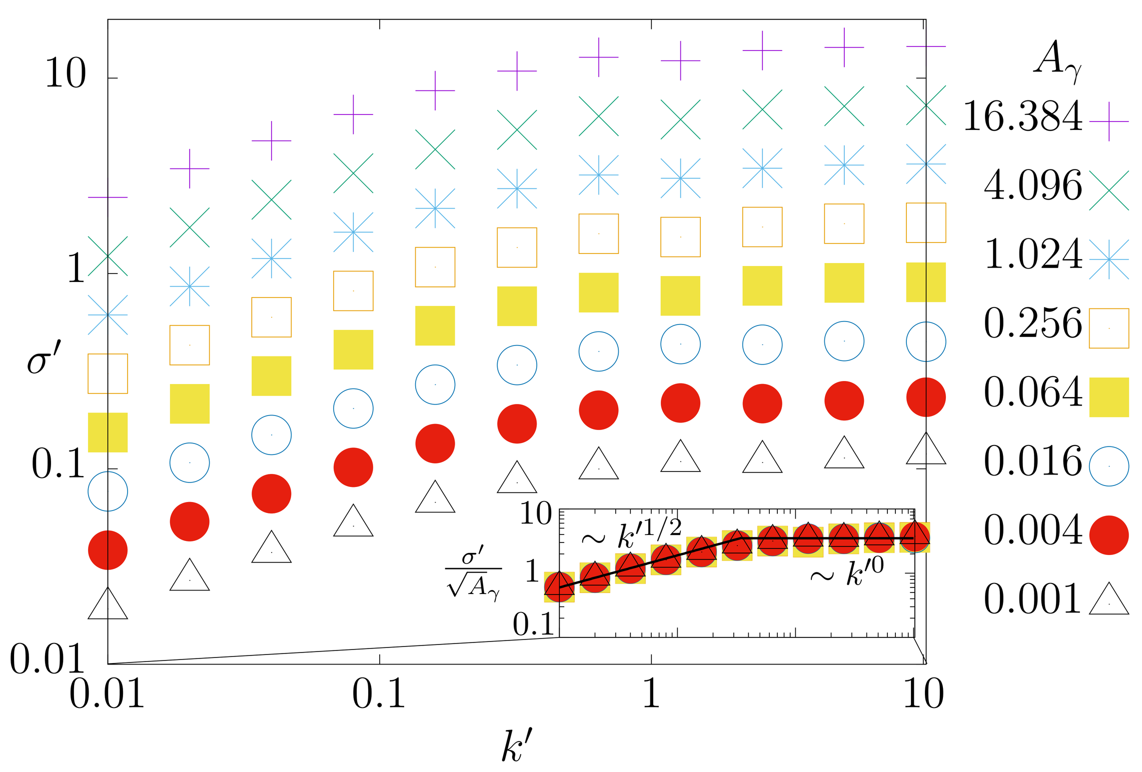

Figure 5. Dispersion relation showing that $\sigma\sim A_\gamma$. There are two regimes of k' dependence, when $k'<1$, $\sigma\sim k'^{1/2}$ and when $k'>1$, $\sigma\sim k'^0$.

$k'<1\quad(\lambda>2\pi L_\mathsf{p})$

Wavelength is larger than the transition region. Scaling behaviour the same as for an infinitesimally thin transition zone.

$$\omega\sim\left(\frac{gk\rho_\mathsf{p}}{\rho_0}\right)^{1/2}$$

$k'>1\quad(\lambda<2\pi L_\mathsf{p})$

Wavelength is shorter than the transition region. Growth rate independent of wavenumber.

$$\omega\sim\left(\frac{g\rho_\mathsf{p}}{L_\mathsf{p}\rho_0}\right)^{1/2}$$